JOURNAL OF BACTERIOLOGY, Oct. 1995, p. 5891–5898 Vol. 177, No. 20
0021-9193/95/$04.00+0
Copyright © 1995, American Society for Microbiology

catM Encodes a LysR-Type Transcriptional Activator Regulating Catechol Degradation in *Acinetobacter calcoaceticus*

CYNTHIA E. ROMERO-ARROYO,[1] MARK A. SCHELL,[1] GEORGE L. GAINES III,[2] AND ELLEN L. NEIDLE[1]*

Department of Microbiology, University of Georgia, Athens, Georgia 30602,[1] and Isogenetics, Inc., Chicago Technology Park, Chicago, Illinois 60612[2]

Received 27 March 1995/Accepted 10 August 1995

On the basis of the constitutive phenotypes of two *catM* mutants of *Acinetobacter calcoaceticus*, the CatM protein was proposed to repress expression of two different loci involved in catechol degradation, *catA* and *catBCIJFD* (E. Neidle, C. Hartnett, and L. N. Ornston, J. Bacteriol. 171:5410–5421, 1989). In spite of its proposed negative role as a repressor, CatM is similar in amino acid sequence to positive transcriptional activators of the LysR family. Investigating this anomaly, we found that insertional inactivation of *catM* did not cause the phenotype expected for the disruption of a repressor-encoding gene: in an interposon-generated *catM* mutant, no *cat* genes were expressed constitutively, but rather *catA* and *catB* were still inducible by muconate. Moreover, this *catM* mutant grew poorly on benzoate, a process requiring the expression of all *cat* genes. The inducibility of the *cat* genes in this *catM* mutant was completely eliminated by a 3.5-kbp deletion 10 kbp upstream of *catM*. In this double mutant, *catM* in *trans* restored muconate inducibility to both *catA* and *catB*. These results suggested the presence of an additional regulatory locus controlling *cat* gene expression. The ability of CatM to function as an activator was also suggested by these results. In support of this hypothesis, in vivo methylation protection assays showed that CatM protects two guanines in a dyad 65 nucleotides upstream of the *catB* transcriptional start site, in a location and pattern typical of LysR-type transcriptional activators. Gel mobility shift assays indicated that CatM also binds to a region upstream of *catA*. DNA sequence analysis revealed a nucleotide near the 3′ end of *catM* not present in the published sequence. Translation of the corrected sequence resulted in the deduced CatM protein being 52 residues longer than previously reported. The size, amino acid sequence, and mode of action of CatM now appear similar to, and typical of, what has been found for transcriptional activators in the LysR family. Analysis of one of the constitutive alleles of *catM* previously thought to encode a dysfunctional repressor indicated instead that it encodes an inducer-independent transcriptional activator.

In the soil bacterium *Acinetobacter calcoaceticus*, the *catM* gene regulates all of the *cat* genes needed for catechol degradation via the β-ketoadipate pathway (Fig. 1) (28). The *cat* genes include *catA*, encoding catechol 1,2-dioxygenase, which converts catechol to *cis*,*cis*-muconate (CCM), and the *catBCIJFD* genes, encoding enzymes for the formation of tricarboxylic acid cycle intermediates from CCM. These genes are clustered on the *A. calcoaceticus* chromosome, with *catM* and two open reading frames separating *catA* from the *catBCIJFD* genes (Fig. 2) (33). In the wild-type strain, *cat* gene expression is induced by CCM, which increases the levels of *cat*-encoded enzymes by approximately 300-fold (2). However, mutants in which some or all of the *cat* genes are constitutively expressed have been isolated. In one such mutant, ADP163, a point mutation that substitutes His for Arg-156 of CatM was found to cause constitutive expression of all of the *cat* genes. This observation and constitutive *catA* expression in the *catM-catB* deletion strain ADP205 contributed to the hypothesis that CatM was a transcriptional repressor of the *cat* genes (28).

In amino acid sequence alignments, the amino-terminal region of CatM aligns well with those of several members of the LysR family of transcriptional activators. In this region, which appears to be involved in the specific binding of the regulators to their target DNA sequences (41), approximately 30% of the CatM residues are identical to those of other LysR proteins (47). The carboxy-terminal region of CatM, however, did not align well with those of other LysR proteins, in part because CatM appeared to be significantly shorter than all other family members (12, 41). Additional analyses of LysR proteins identified a region likely to be involved in inducer-compound recognition and/or binding (41). Although an inducer is normally necessary for transcriptional activation, several mutations cause the production of inducer-independent LysR activators. Single amino acid substitutions near residue 150 of several LysR proteins lead to constitutive expression of the target genes (41). Because this position is close to that of the substitution which causes constitutive gene expression in the *catM* mutant ADP163, we reconsidered the roles of the wild-type and mutant CatM proteins in the regulation of *cat* gene expression.

Analysis of an *A. calcoaceticus* mutant in which we inactivated *catM* by interposon insertion clearly showed that CatM does not repress its regulated targets. Other experiments, including in vivo footprinting to localize the CatM binding sites within the regulated *catB* promoter, suggested that CatM, like most other LysR-type proteins, functions predominantly as a transcriptional activator. Consistent with this role of CatM, *catM* of ADP163 was found to encode an inducer-independent transcriptional activator. During these analyses, we obtained evidence for an additional *cat* gene regulator whose presence may have obscured the role of CatM in previous studies.

MATERIALS AND METHODS

Bacterial strains and plasmids. *A. calcoaceticus* strains and plasmids are described in Table 1 and Fig. 2. Bacteria were cultured in Luria broth (LB) and

* Corresponding author. Phone: (706) 542-2852. Fax: (706) 542-2674. Electronic mail address: eneidle@uga.cc.uga.edu.

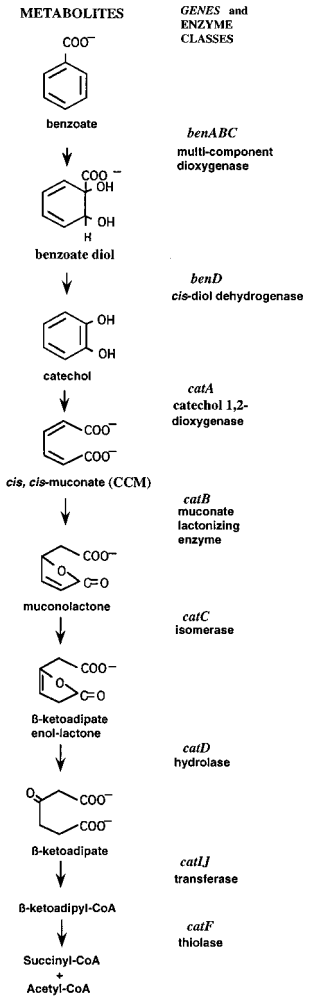

FIG. 1. Metabolites, structural genes, and enzymes associated with dissimilation of benzoate via the β-ketoadipate pathway. CoA, coenzyme A.

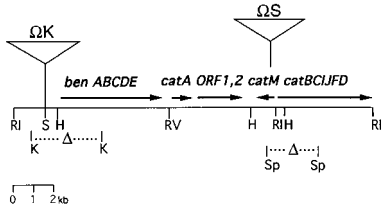

FIG. 2. Physical and genetic map of the chromosomal *A. calcoaceticus ben-cat* region. The locations of genes are shown relative to some of the known restriction endonuclease sites: *Eco*RI (RI), *Eco*RV (RV), *Hin*dIII (H), *Kpn*I (K), *Sal*I (S), and *Sph*I (Sp). Arrows indicate transcriptional directions. The position of the Km^r cassette inserted upstream of *benA* is indicated (ΩK), as is the position of the Sm^r Sp^r cassette inserted in *catM* (ΩS). The positions of the 1.5-kbp *catM-catB* deletion (Sp. . .Δ. . .Sp) and the 3.5-kbp *ben* deletion (K. . .Δ. . .K) are indicated.

minimal media at 37°C as previously described (39, 43). All *A. calcoaceticus* strains were derived from BD413 (15, 16), which we designate ADP1. The following *Escherichia coli* strains were used as plasmid hosts: JM83 (50), JM101 (50), S17-1 (44), MC1061 (48), and SK6501 (9). For interposon mutagenesis, we used either the 2-kbp Ω fragment (ΩS) from pHP45 (36) which encodes resistance to streptomycin (Sm^r) and spectinomycin (Sp^r) or the 2-kbp Ω fragment (ΩK) of pUI1637 (7) encoding kanamycin resistance (Km^r). Plasmids carrying Ω cartridge *cat* gene disruptions were linearized with restriction endonucleases and used for specific alteration of the *A. calcoaceticus* chromosome as previously described (28). Plasmid pRA3030 was generated by transposon mutagenesis of *E. coli* SK6501(pIB25) with lambda B20 Tn*5*::*lacZ* (9, 45). The location of *lacZ* was determined by restriction digest analysis.

DNA manipulations and Southern analysis. Chromosomal and plasmid DNA purifications, subcloning, transformations, and Southern hybridization analyses were performed by standard methods (39). DNA probes for Southern hybridization analyses were labeled with digoxigenin by random priming, and probes were detected with anti-digoxigenin alkaline phosphatase conjugates and chemiluminescent substrates according to the instructions of the Genius System (Boehringer Mannheim Corp., Indianapolis, Ind.).

CatA and CatB assays. Cultures were diluted 1:3 in fresh LB medium and grown for 2 to 3 h in the presence or absence of inducers, 3 mM benzoate, or 3 mM CCM. Cell extracts were prepared by sonication (43), and protein concentrations were determined by the method of Bradford (1), with bovine serum albumin as the standard. Catechol 1,2-dioxygenase, encoded by *catA*, and muconate-lactonizing enzyme, encoded by *catB*, were assayed spectrophotometrically by monitoring the increase or decrease in CCM concentration, respectively, as indicated by A_{260} (31, 32).

β-Galactosidase assays. *E. coli* cells were harvested after reaching an A_{600} of 0.6, washed once, and suspended with buffer containing 10 mM Tris-HCl (pH 7.6), 8 mM $MgSO_4$, and 1 mM K_2PO_4. Cell suspensions were sonicated twice for 30 s at 4°C, and cell debris was removed by centrifugation. Cell supernatant extracts were assayed for β-galactosidase activity as described by Miller (26), and protein concentrations were determined by the method of Kalb and Bernlohr (17).

DNA sequence analysis. The DNA sequence of pIGG9 was determined with a double-stranded plasmid template and an ABI373A automated DNA sequencer (Applied Biosystems, Inc., Foster City, Calif.). DNA sequences were analyzed with programs of the Wisconsin Genetic Computer Group (GCG) (6) or the IG molecular biology software system (IntelliGenetics, Inc., Mountain View, Calif.).

Gel retardation DNA-protein binding assays. DNA-protein complexes were analyzed by gel electrophoresis as described by Fried and Crothers (8), with the modifications of Schell and Poser (42) being used, except that the incubation buffer (10 mM Tris-HCl [pH 7.6], 1 mM EDTA, 50 mM KCl, 5 mM dithiothreitol) contained 0.3 mg of bovine serum albumin per ml and 0.4 mg of sonicated salmon sperm DNA per ml. Cell extracts were prepared, and protein content was determined as described above for the β-galactosidase assays, except that incubation buffer was used for cell sonication. Restriction fragments used as binding substrates were purified by polyacrylamide gel electrophoresis. DNA was removed from gel fragments by electroelution and then labeled with Klenow fragment and [α-^{32}P]dATP (39). The labeled DNA fragments (4,000 cpm per reaction) were mixed with 0.1 to 2.5 μg of cell extract protein in a total volume of 15 μl, incubated at 37°C for 15 min, and then electrophoretically separated on 6% polyacrylamide gels. DNA migration was monitored by autoradiography.

Determination of the *catB* transcription start site by primer extension. Total *A. calcoaceticus* RNA was isolated as described by Williams and Rogers (49), and the 5′ ends of the *catB* mRNA transcripts were mapped as described by Delic et al. (5). The oligonucleotide primer, 5′-TCCACTGATTTATACATCGG-3′ (primer B), was complementary to the first 17 nucleotides of the *catB* coding sequence as well as 3 nucleotides upstream of the ATG translational start codon. This primer was labeled at its 5′ end with [γ-^{32}P]ATP and T4 polynucleotide kinase (39). The oligonucleotide (2×10^5 cpm) was annealed with 50 μg of RNA in 20 μl of 50 mM Tris-HCl (pH 8.0) and 100 mM KCl after the mixture was heated at 90°C for 1 min, 60°C for 2 min, and then 4°C for 15 min. The resultant hybrids served as templates in extension reactions at 42°C for 50 min with 10 U of avian myeloblastosis virus reverse transcriptase, 0.5 mM deoxynucleoside triphosphates, and 6 U of RNasin ribonuclease inhibitor (Promega Corp., Madison, Wis.) (39). The same labeled oligonucleotide was used in parallel dideoxy chain termination sequencing reactions with pRA316 template DNA to generate a size standard sequence ladder. Products were analyzed on 5% polyacrylamide–urea gels.

In vivo footprint analysis with DMS. Footprint analysis was carried out by the method of Gralla (11) as modified by Huang and Schell (14). Recombinant plasmids with the *catB* promoter of *A. calcoaceticus* were methylated with dimethylsulfate (DMS) in vivo in *E. coli* strain JM83 in the presence and absence of *catM*. Methylated plasmid DNA was purified and cleaved with piperidine, and the cleavage products were analyzed by primer extension with Sequenase version 2.0 (U.S. Biochemical Corp., Cleveland, Ohio). A ^{32}P-labeled oligonucleotide, 5′-ATCTGAGGTGTCTTAGTTCC-3′ (primer M), complementary to bases 2 to 22 of the *catM* coding sequence and a second labeled oligonucleotide (primer B, described above for transcript mapping) were used for analysis of the sense (bottom) strand and the antisense (top) strand, respectively.

Nucleotide sequence accession number. The corrected DNA sequence of *catM* has been deposited with GenBank under accession number M76991.

RESULTS

Construction and characterization of *catM* insertion mutants ISA13 and ISA35. Although the hypothesis that CatM represses *cat* gene expression was consistent with the constitu-

TABLE 1. Bacterial strains and plasmids

Strain or plasmid	Relevant characteristic(s)	Reference or source
A. calcoaceticus		
ADP1	Wild type (BD413)	15 and 16
ADP163	*pcaE3125 catM3102*	28
ADP205	Δ(*catM-catB3205*)	28
ISA13	*catM*::ΩS *4013*	This study
ISA21	Δ(*benM-benC4021*)	This study
ISA35	Δ(*benM-benC4021*) *catM*::ΩS *4013*	This study
ACN10	*benM*::ΩK *5008* Δ(*catM-catB3205*)	This study
Plasmids		
pUC13 and pUC19	Ap^r	50
pTZ18U	Ap^r	25
pRK415	Tc^r	20
pIB15[a] and pIB16[b]	1.3-kb *Hin*dIII *catM* fragment in pUC19	28
pIB25[a]	1.3-kb *Hin*dIII *catM* fragment in pRK415	28
pIB27[a]	1.3-kb *Hin*dIII *catM3102* fragment in pRK415	This study
pIGG9	*Eco*RI-*Hin*dIII *catM*::ΩS fragment in pUC19	This study
pIGG16	*Eco*RI-*Eco*RV *ben* fragment with Δ(3.5-kb *Kpn*I) in pRK415	This study
pIGG19	*Stu*I-*Hin*dIII *catM* fragment in pUC19	This study
pRA316	*Eco*RI-*Hin*dIII *catM-catB* region in pTZ18U	This study
pRA3030	*catM*::Tn*5lacZ B20* in pIB25	This study
pBAC12	1.9-kb *Eco*RI-*Hin*dIII *ben*-::ΩK in pUC19	This study

[a] *catM* allele transcriptionally controlled by the *lac* promoter of the vector.
[b] *catM* allele transcribed in the opposite orientation relative to that of the *lac* promoter of the vector.

tive phenotypes of two *catM* mutants, ADP163 and ADP205 (28), the possibility that CatM regulates by other mechanisms could not be eliminated by previous studies. Whereas *catA* is constitutively expressed in *catM* mutant strain ADP205, the deletion also encompasses the *catB* gene, making the specific role of *catM* in the resultant phenotype unclear. To further evaluate the function of CatM, we inactivated the genomic copy of *catM* by Ω interposon mutagenesis (36), leaving the *catBCIJFD* gene cluster intact. First, we constructed pIGG9, which has a 2-kbp ΩS cartridge (a Sp^r cassette with flanking transcriptional and translational stop signals) inserted in the *Sph*I site of *catM* (Fig. 2). The pIGG9 DNA was then linearized with *Eco*RI and used to transform the wild-type strain ADP1. An Sp^r transformant, designated ISA13, was isolated, and Southern hybridization analysis confirmed that in it, the *catM*::ΩS allele replaced the chromosomal wild-type *catM*.

In contrast to the previous *catM* mutants, ISA13 did not express the *cat* genes constitutively. The *catM* disruption only slightly reduced the maximal expression of *catA* and *catB* in response to CCM (Table 2). However, the ability of benzoate or its metabolites to induce *catB* expression was reduced fivefold by *catM* disruption (Table 2). This is consistent with the reduced ability of ISA13 to metabolize benzoate. Whereas both the wild-type strain and the constitutive mutant ADP163 utilize benzoate as the sole carbon source, each with a doubling time of 60 to 90 min, the *catM* disruption of ISA13 resulted in 3.5 times slower growth on benzoate. These results suggested that CatM does not negatively regulate expression of the *cat* genes. In ISA13, the ability to induce *catA* and *catB* expression appeared to be mediated by a regulator(s) other than CatM, since as described below, the presence of a 3.5-kbp deletion 10 kbp upstream of *catM* in a *catM*-disrupted mutant eliminated all inducible *catA* and *catB* expression.

Strains blocked in the metabolism of benzoate have been used to show that benzoate itself induces *cat* gene expression (29). In order to determine whether benzoate alone was responsible for CatA and CatB induction in ISA13 (Table 2), it was necessary to block its metabolism to CCM. The *benABC* genes, involved in the initial step of benzoate catabolism (30) (Fig. 1), were first deleted from a *ben* gene-carrying plasmid by the removal of a 3.5-kbp *Kpn*I fragment, generating pIGG16. This *ben* deletion was transformed into the genome of ADP1 by linearizing pIGG16 with *Bam*HI, mixing the DNA with wild-type ADP1 cells, and screening the transformants for the loss of the ability to utilize benzoate as the sole carbon source, thereby generating strain ISA21. ISA21 was further trans-

TABLE 2. Inducible expression of *catA* and *catB* in the *A. calcoaceticus* wild type and *catM* mutants

Strain	Relevant characteristic(s)	Sp act (nmol/min/mg of protein) induced by growth with[a]:					
		No inducer		Benzoate[b]		CCM	
		CatA	CatB	CatA	CatB	CatA	CatB
ADP1	Wild type	<5	<10	393	190	167	230
ISA13	*catM*::ΩS *4013*	<5	<10	237	43	93	193
ISA35	Δ(*ben-benC4025*) *catM*::ΩS *4013*	<5	<10	<5	<10	<5	<10
ISA35(pIB25)	*catM* in *trans*	<5	<10	<5	<10	80	150

[a] Values are averages of at least three repetitions, with standard deviations of <20%. Cells were grown in LB with either 3 mM benzoate or 3 mM CCM as an inducer.
[b] In ADP1 and ISA13, benzoate can be metabolized to CCM.

formed to Sp^r by the same method with linearized pIGG9 which contains the *catM*::ΩS allele. Southern hybridization analysis confirmed that the genome of the resultant strain ISA35 carries both the ΩS insertion in *catM* and the *ben* deletion (including *benABC* and an additional 1-kbp region upstream of *benA*).

In addition to blocking the conversion of benzoate to CCM, the *ben* deletion in ISA35 unexpectedly eliminated all induction of *catA* and *catB* by either benzoate or CCM (Table 2; compare ISA35 to ISA13). This result suggests that a locus in the deleted *ben* region controls the expression of *catA* and *catB* in ISA13. In the absence of this regulatory locus, plasmid pIB25, carrying only wild-type *catM*, restored the CCM inducibility of both *catA* and *catB* but did not restore the induction of *catA* by benzoate in strain ISA35 (Table 2). CatM, therefore, appeared to be responsible for transcriptional activation of both *catA* and *catB* in response to CCM. These results further argue against a role for CatM as a repressor of *catA* and *catB* expression.

Reanalysis of the *catM* DNA sequence. Previous DNA sequence data (28) implied both that the CatM protein was much smaller than any other LysR-type regulator and that it lacked conserved carboxy-terminal domains likely to be involved in transcription activation (41). Therefore, the sequence of *catM* near the published termination codon of the *catM* open reading frame was again determined, with plasmid pIGG19 (Table 1) being used as the template. An additional C nucleotide was found 17 nucleotides upstream of the original stop codon. Starting at nucleotide 738, with position 1 being the first nucleotide of the *catM* coding region, the sequence was found to be TGCCATGG rather than the published TGCATGG. This sequence correction predicts an *Nco*I recognition site at position 740; the presence of this corrected sequence was confirmed by digestion of pIGG19 with *Nco*I.

This sequence correction resulted in the extension of the *catM* open reading frame by 156 nucleotides and extension of the deduced amino acid sequence by 52 residues. This new 303-residue CatM is very similar in size and sequence to other LysR-type activators. In sequence alignments of CatM with each of the LysR activators—CatR (37), TfdR (24), ClcR (4), TcbR (46), and BphR (21)—the identity of the aligned residues ranged from 28 to 41% (similarity between 50 and 60%). These proteins are involved in the regulation of aromatic compound degradation by diverse bacteria, and each controls the expression of genes that are either the same as or similar to those regulated by CatM of *A. calcoaceticus*. CatM was most similar to CatR of *Pseudomonas* species (13, 37), with the new 52 C-terminal CatM residues showing 45% similarity to those of the homologous CatR region.

CatM specifically binds to the *catM-catB* intercistronic region and to a region upstream of *catA*. To obtain additional evidence that CatM directly activates transcription from the *catB* promoter, we used gel retardation assays. A 313-bp *Eco*RI-*Hin*dIII fragment containing the *catM-catB* intercistronic region (Fig. 3A) was end labeled with ^{32}P and incubated with cell extracts of *E. coli* JM83 either carrying plasmids with *catM* transcriptionally controlled by the vector's *lac* promoter (pIB15) or with *catM* in the opposite orientation relative to the *lac* promoter (pIB16) or carrying no plasmid. The electrophoretic mobility of the *catM-catB* intercistronic DNA fragment was retarded only when it was preincubated with crude extracts of *catM*-containing cells (Fig. 3B). Increasing concentrations of crude extracts from *E. coli* JM83(pIB15) or *E. coli* JM83(pIB16) caused an increasing amount of the fragment to show retarded mobility. Electrophoretic mobility shifts of the labeled fragment were not significantly affected by 0.1 to 10 mM inducer CCM added to the binding reactions prior to electrophoretic separations (data not shown). The lack of an obvious effect of the inducer on apparent DNA binding by CatM is consistent with behavior reported for other LysR proteins that are transcriptional activators (41).

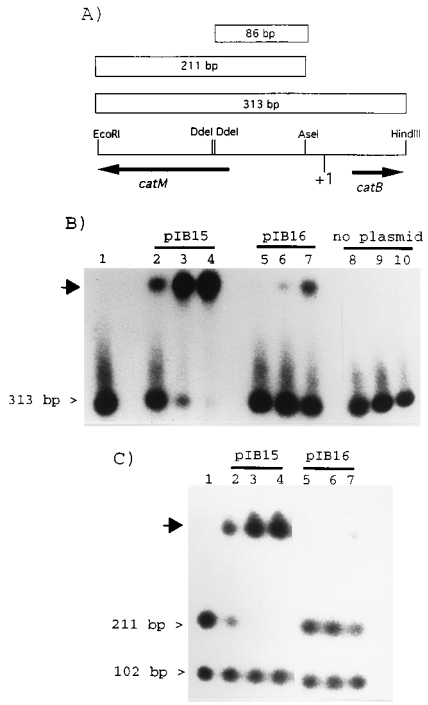

FIG. 3. Gel retardation assays of CatM binding to the *catM-catB* intercistronic region. (A) Restriction map of the 313-bp *Eco*RI-*Hin*dIII fragment carrying 135 and 54 bp, respectively, of the *catM* and *catB* coding sequences and the intergenic region. Arrows show the directions of *catM* and *catB* transcription and the approximate location of the portions of the respective coding regions contained on this fragment. The +1 indicates the transcript initiation site of *catB*. Rectangles show fragments whose mobilities were shifted by CatM. (B) Autoradiogram following electrophoresis of the end-labeled *Eco*RI-*Hin*dIII fragment incubated in a total volume of 15 μl with cell extracts (lane 1, no addition; lanes 2, 5, and 8, 0.1 μg of protein; lanes 3, 6, and 9, 0.3 μg of protein; lanes 4, 7, and 10, 0.9 μg of protein) from *E. coli* JM83 (pIB15) (lanes 2 to 4), JM83 (pIB16) (lanes 5 to 7), and JM83 (lanes 8 to 10). A solid arrow marks the position of DNA fragments which are retarded by incubation with cell extracts. (C) The *Eco*RI-*Hin*dIII fragment was digested with *Ase*I, end labeled, and incubated with 0 μg (lane 1), 0.3 μg (lanes 2 and 5), 0.8 μg (lanes 3 and 6), and 2.3 μg (lanes 4 and 7) of protein from the same cell extracts as in panel B.

To further localize DNA sequences that specifically interact with CatM, the 313-bp *Eco*RI-*Hin*dIII fragment was digested with *Ase*I, and the mixture was ^{32}P end labeled. The mixture of the two labeled fragments was then incubated with the same crude extracts described above. The 211-bp *Eco*RI-*Ase*I fragment showed retarded migration when it was incubated with extracts from cells harboring plasmids with *catM*, indicating that CatM binds to this fragment (Fig. 3C). Extracts from cells carrying pIB15 show greater binding activity than those from cells carrying pIB16, most likely because the *A. calcoaceticus* DNA fragment is oriented so that the *lac* promoter of pIB15 drives *catM* expression. The *lac* promoter drives higher *catM* expression than does the *catM* promoter alone, which appears to be weakly expressed in *E. coli*. Protein binding to the 211-bp *Eco*RI-*Ase*I fragment was sequence specific, because migration of the 102-bp *Ase*I-*Hin*dIII fragment was unaffected by incubation with any of the crude extracts tested (Fig. 3C).

To more precisely locate the sequence binding CatM, the mixture of the labeled *Eco*RI-*Ase*I and *Ase*I-*Hin*dIII fragments

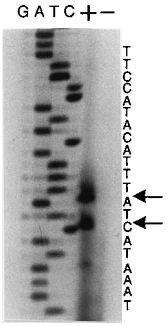

FIG. 4. Mapping of the 5′ end of *catB* transcripts. Primer extension reactions were carried out with a ^{32}P-labeled, *catB*-specific oligonucleotide (primer B) and RNA from wild-type ADP1 grown in LB with either 5 mM benzoate (+, induced) or 10 mM succinate (−, noninduced). The same oligonucleotide was used to generate the sequencing ladder (lanes G, A, T, and C). The arrows show the major cDNA products and indicate *catB* transcript initiation sites 26 to 28 bp upstream of the *catB* ATG translation initiation codon on the coding strand.

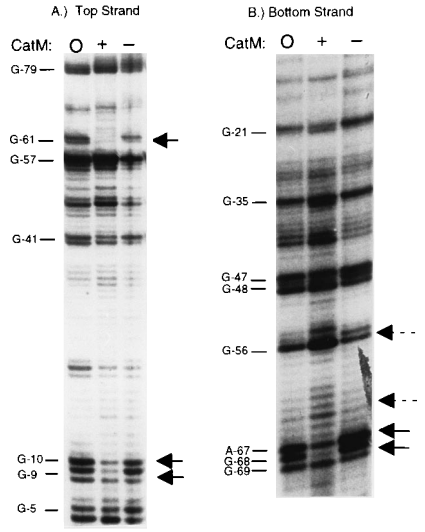

FIG. 5. In vivo footprinting analysis of CatM binding to the *catB* promoter. *E. coli*(pRA316) (CatM$^-$) and *E. coli*(pIB16) (CatM$^+$) were grown in LB and methylated with DMS. Plasmid DNA was purified and cleaved with piperidine, and the fragments were analyzed by primer extension with labeled primer B for the top strand (A) and labeled primer M for the bottom strand (B). For lanes O, purified native pIB16 was first methylated in vitro with DMS. The G and A numbers at the left indicate the positions of reactive guanines and adenines in the promoter region relative to the transcript start site (+1). Solid arrows indicate protected bases whose methylation was specifically inhibited by the presence of CatM. The dotted arrows mark bases whose methylation was enhanced by the presence of CatM.

was digested with *Dde*I and used as a binding substrate. Only the 86-bp *Dde*I-*Ase*I fragment (Fig. 3A) showed a mobility shift dependent on preincubation with crude extracts containing CatM (data not shown), indicating that the CatM binding site in the *catB-catM* intercistronic region lies between the *Dde*I and *Ase*I sites. Similarly, a labeled fragment carrying 388 bp between the *Ssp*I and *Sal*I restriction sites and ending 52 bp upstream of the *catA* coding region was preincubated with cell extracts of *E. coli* JM83(pIB15), and this retarded its electrophoretic mobility (data not shown). Preincubation with extracts from *E. coli* JM83 had no effect, indicating that CatM also binds to a specific sequence upstream of *catA*.

Localization of the transcription start site and promoter of *catB*. The results outlined above showed that CatM binds to an 86-bp region located 48 bp upstream of the *catB* translation start site, a region also likely to contain the *catB* promoter. The position of the CatM binding site relative to that of the promoter elements should give insight into how it regulates *catB* expression. Thus, we localized the *catB* transcriptional start site by primer-extension techniques: total RNA was prepared either from wild-type *A. calcoaceticus* cells induced for CatB production by growth in LB with benzoate or from uninduced cells grown in LB with succinate. RNA samples annealed with a ^{32}P-labeled, *catB*-specific primer served as templates for reverse transcriptase-mediated extension reactions. cDNAs were detected only in the presence of RNA isolated from induced cultures (Fig. 4), indicating that increased *catB* expression in response to benzoate and/or its metabolic descendants occurs at the transcriptional level. The majority of benzoate-induced *catB* transcripts started between 26 and 28 nucleotides upstream of the ATG-methionine translational initiation codon (Fig. 4).

In vivo interactions between CatM and nucleotides of the *catM-catB* intercistronic region. Next, we used in vivo methylation protection analysis to define specific nucleotides involved in CatM binding. DMS methylates the N-7 of guanines and, at a lower rate, the N-3 of adenines; this methylation can be dramatically inhibited or enhanced if the bases are interacting with a protein (11, 40). The strength and position of such interactions can be investigated by comparing the base cleavage products of target DNA treated with DMS in the presence and absence of a DNA-binding protein.

Cultures of *E. coli* cells containing a plasmid with either the *catM-catB* intercistronic region and the complete *catM* gene (pIB16) or with the *catM-catB* intercistronic region and only the first 135 bp of *catM* (pRA316) were treated with DMS. Plasmid DNA was isolated and cleaved at methylated sites with piperidine. Methylation patterns were determined by analyzing the cleavage fragments by means of primer extension reactions (Fig. 5). The presence of CatM specifically caused strong protection of a guanine at position −61 (relative to the +1 *catB* transcription initiation site) on the antisense (top) strand (G-61) (Fig. 5A). Similarly, a guanine and an adenine at −68 and −67, respectively, on the sense (bottom) strand were protected from methylation, again only in the presence of CatM (G-68 and A-67) (Fig. 5B). A guanine at position −56 (and possibly one at −57) as well as several adenines between −66 and −62 showed increased methylation caused by the presence of CatM.

These results indicated that CatM interacts with nucleotides centered around position −65 of the *catB* promoter. This CatM-binding region (−72 to −58) contains an interrupted dyad (ATAC-N$_7$-GTAT) whose position and methylation protection pattern are similar to those that have been observed for other LysR-type transcriptional activators, including CatR and ClcR, which control the aromatic degradation genes with a similar function in *Pseudomonas* spp. (4, 34, 35, 41). Addition of the inducer CCM to the *E. coli* cultures prior to methylation with DMS did not consistently produce any new changes in the protection pattern. However, the permeability of *E. coli* to CCM is not known, and thus the effects of the inducer on CatM interactions with its binding site remain unclear. Finally, guanines at −10 and −9 on the antisense strand showed consistent protection from DMS methylation only in the presence of CatM.

CatM negatively autoregulates. The CatM binding site identified above is 23 bp upstream of the *catM* translational start codon and thus is likely to be near the *catM* promoter. On the basis of similarity to other LysR systems, we expected that the

TABLE 3. Expression of *catA* and *catB* with wild-type or mutant *catM* alleles in *trans*

Strain	Relevant characteristic	Sp act (nmol/min/mg of protein) of LB-grown cells[a]	
		CatA	CatB
ADP163	*catM3102* (constitutive allele)	153	927
ADP1	Wild type	<5	<10
ADP1(pIB25)	Wild-type *catM* in *trans*	<5	<10
ADP1(pIB27)	*catM3102* in *trans*	103	333

[a] Values are averages of at least three repetitions, with standard deviations of <20% of the values shown.

binding of CatM at this site should reduce its own transcription. To evaluate this, we analyzed the expression of a plasmid-borne *catM*::*lacZ* fusion on pRA3030 in *E. coli* MC1061 both in the presence and in the absence of *catM* on pIB15. The β-galactosidase activity directed from the *catM*::*lacZ* fusion, 51 Miller units, was reduced by threefold to 15 Miller units when *catM* was placed in *trans*. Thus, like many other LysR transcriptional activators (41), *catM* is negatively autoregulated.

Explanation of the constitutive phenotypes of mutants ADP163 and ADP205. All the data presented above are consistent with the hypothesis that CatM acts as a transcriptional activator. To determine how the point mutation in *catM* of ADP163 caused high *catA* and *catB* expression in the absence of inducers, we cloned the 1.3-kb *Hin*dIII fragment containing this allele into a broad-host-range plasmid, forming pIB27. The presence of pIB27 in *trans* in wild-type ADP1 caused constitutive *catA* and *catB* expression (Table 3) consistent with the idea that *catM* in ADP163 encodes a *trans*-dominant, inducer-independent CatM activator, not an inactive repressor.

High CatA levels in *catM-catB* deletion mutant ADP205 had been attributed to the deletion of *catM* (28), although here we found that specific disruption of *catM* did not cause the same effect. Because a regulatory locus in the *ben* region appeared to affect *catA* expression in ISA13, we tested the possibility that this region was involved in the constitutive expression of *catA* in ADP205. Interposon mutagenesis was used to disrupt the putative regulatory locus: plasmid pBAC12 (Table 1) carrying an ΩK cassette (7) immediately upstream of *benA* was linearized and used to transform ADP205 to Km^r. Southern hybridization confirmed the presence of both the ADP205 *catM-catB3205* deletion and the *ben*::ΩK insertion in the resultant strain ACN10 (Fig. 2). Constitutive expression of *catA* in ADP205 was eliminated by introduction of the *ben*::ΩK insertion; the specific activity of CatA (catechol 1,2-dioxygenase) in LB-grown ACN10 was <5 nmol/min/mg of protein, compared with a value of 250 nmol/min/mg of protein determined for similarly grown ADP205 cultures. This suggests that CatM is not the sole regulator of *catA*, and therefore the constitutive phenotype associated with the *catM-catB* deletion results from events other than the repression of *catA* by CatM. The possible involvement of the *catB* deletion in causing the constitutive *catA* expression of ADP205 is discussed below.

DISCUSSION

CatM activates *cat* gene expression. Three lines of evidence demonstrated that *A. calcoaceticus* CatM is a LysR-type regulator that activates, rather than represses, *cat* gene expression. First, in a *ben*-deleted background, inactivation of *catM* caused a loss of muconate-inducible *catA* and *catB* expression that was specifically restored by *catM* in *trans*. Second, analysis of the DNA-protein interactions of CatM with the *catB* promoter showed that the position and DNA sequence of regions which interact with CatM are characteristic of those involved in LysR-type transcriptional activation. Third, the *trans*-dominant nature of the ADP163 *catM* allele which causes constitutive *cat* gene expression indicated that it encodes a mutant CatM protein that is an inducer-independent activator, not a dysfunctional repressor.

Analysis of a revised *catM* DNA sequence showed that CatM is a 303-residue protein, very similar in size and amino acid sequence to many other LysR transcriptional activators. Strong homology (41% identity and 60% similarity) to CatR, a transcriptional activator of *Pseudomonas* sp. *catB*, a gene which is isofunctional to *A. calcoaceticus catB* (13, 37, 38), was detected. The DNA sequences of *catM* and *catR* are 45% identical, despite significant differences in G+C content; *catM* contains 44% G+C, in contrast to *catR*, which contains 65% G+C. This degree of homology strongly suggests a common ancestry for both genes. Both CatM and CatR appear to be members of a subfamily of LysR activators, including ClcR (3, 4), TcbR (46), TfdR (18, 24), and TfdS (19, 24). Members of this subfamily regulate genes encoding muconate- or chloromuconate-lactonizing enzymes and/or genes encoding oxygenases that act on catechol or chlorinated aromatic compounds from *Acinetobacter*, *Pseudomonas*, and *Alcaligenes* species.

Sequences involved in the binding of many of these LysR-type regulators to their target DNA regions have been identified (3). Characteristic of LysR-type binding sites is a T-N_{11}-A motif and a small region of interrupted dyadic symmetry centered approximately 65 nucleotides upstream of the regulated transcriptional start sites (3, 10). Exactly such a sequence, ATAC-N_7-GTAT, is present at the *A. calcoaceticus catB* promoter in the region identified by in vivo footprinting as the likely CatM recognition and binding site (Fig. 6). This sequence is nearly identical to those proposed as the binding sites of CatR, ClcR, TfdR, and TcbR (3, 22, 35). Additionally, the two guanines of the dyad which we showed by in vivo footprinting to be involved in the binding of CatM to the *A. calcoaceticus catB* promoter are at the same locations as ones which have been shown by site-directed mutagenesis and meth-

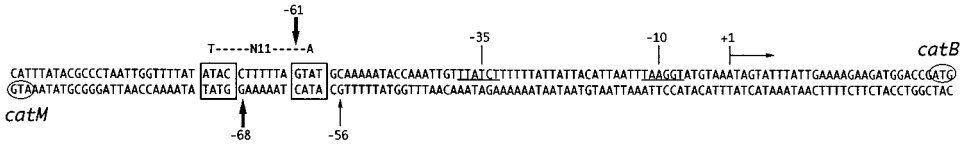

FIG. 6. Structure and position of the CatM binding site in the *catM-catB* intercistronic region. The ATG translation initiation codons for the divergently transcribed *catM* and *catB* genes are circled. Possible −35 and −10 sequences of the *catB* promoter are underlined, and the *catB* transcription start site is indicated (+1→). Nucleotides (G-68 and G-61) protected from methylation by CatM are marked with thick vertical arrows. The G-56 nucleotide whose reactivity to DMS is increased by CatM is marked with a thin arrow. The dyadic elements of the proposed CatM binding site are boxed, and T-N_{11}-A shows the position of a motif that is characteristic of the binding sites of LysR-type regulators.

ylation interference to be important for binding and/or transcriptional activation of the *Pseudomonas catB* promoter by CatR (35). We did not observe any interactions between CatM and guanines downstream of the −65 binding site, even in the presence of its inducer. For many LysR-type activators, including CatR, inducer-dependent interactions with nucleotides downstream of the primary binding site, near position −40, have been reported (35, 38). The failure to observe such interactions may result from the low permeability of *E. coli* to the inducer CCM, the low number of available guanines in this region of the *catB* promoter, or different mechanisms of action. The sequences of the *catB* promoter downstream of the CatM binding site (−55 to +1) in *A. calcoaceticus* differ extensively from those downstream of the CatR binding site in *Pseudomonas putida*, suggesting fundamental differences in promoter structures and RNA polymerase binding sites. Moreover, we observed apparent CatM-dependent protection of guanines at positions −9 and −10, which, although atypical for LysR-type regulators, may suggest DNA bending by CatM, a possibility supported by the presence of A tracts in the promoter region. It is also possible that this CatM-dependent protection of guanines close to the *catB* transcriptional start site might reflect aberrant sequestration of RNA polymerase at the *catB* promoter (23). Nonetheless, conservation of the upstream sequences involved in the binding of CatM, CatR, and ClcR indicates a common ancestry not only for the genes encoding the homologous activators, all of which respond to similar inducer compounds, but also for the cognate regulatory sites.

A regulator distinct from CatM regulates *catA* in response to benzoate and CCM. Although we clearly showed that CatM can activate *cat* gene expression, simple disruption of *catM* in strain ISA13 had only a slight effect on the inducible expression of *catA* and *catB*. Moreover, inducible expression of *catA* in response to either benzoate or CCM in a strain which lacks *catM* and which cannot further metabolize either inducer was observed (28). These results suggest the existence of a *cat* gene regulator(s) distinct from CatM. In the presence of such a regulator, the overlapping ability of *catM* to activate *cat* gene expression is obscured. The *ben* deletion in conjunction with the *catM* disruption in strain ISA35 eliminated all inducible expression of *catA* and *catB*, thereby allowing us to examine the role of *catM* by placing it in *trans*. The ability of *catM* to restore CCM-inducible but not benzoate-inducible *cat* gene expression in this strain indicated that CatM responds to CCM but not to benzoate.

The 3.5-kbp *ben* region deletion in ISA35 eliminated all of the *catM*-independent regulation of *catA* and *catB*, suggesting that the deletion contains a regulatory region affecting the expression of *catA* and *catB*. Consistent with this, insertion of an ΩS or ΩK cartridge in a region just upstream of *benA* also eliminated the inducibility of *catA* in response to benzoate (27). Finally, when the ΩK cartridge was introduced in the same *ben* region of the ADP205 chromosome, it eliminated the constitutive *catA* expression caused by the chromosomal *catM-catB* deletion. Although high *catA* expression in ADP205 was originally attributed to the loss of *catM*, it now seems more likely that the constitutive phenotype results from the loss of *catB*, since we have observed constitutive *catA* expression in a *catB*-deleted strain which has a wild-type *catM* (27). One possible explanation is that the deletion of *catB* causes CCM accumulation, perhaps from the metabolism of endogenous aromatic compounds such as anthranilate, and that CCM thus generated can cause the *ben* region regulator to activate *catA* expression.

Reanalysis of the constitutive mutant ADP163. Although here we found that the *catM3102* allele carried on pIB27 was dominant with respect to that of the wild type and caused constitutive *catA* and *catB* expression in ADP1 (Table 3), previous experiments showed the opposite: wild-type *catM*, in *trans* on pIB25, in ADP163 eliminated constitutive *cat* gene expression (28). Thus, it appears that in these merodiploids, *cat* gene expression depends on which *catM* allele is plasmid borne, implicating gene dosage in this effect. It is also possible that the ratio of the constitutive and the wild-type *catM* gene products affects the formation or the levels of functional CatM oligomers. The possibility that the phenotype of these strains results from the formation of aberrant CatM hetero-oligomers is consistent with the recent observation that the presence of the wild-type *catM* in *trans* in the constitutive ADP163 mutant not only eliminated the constitutive expression of *catA* and *catB* but also prevented high induced levels of *catA* and *catB* expression in response to CCM and benzoate (27). Although CatR appears to function as a dimer (35), the subunit structure of active CatM remains to be determined.

ACKNOWLEDGMENTS

This research was supported by NIH grants GM32255 (to M.A.S.) and SBIR IR43ESO6304 (to G.L.G.). Additional support was provided by National Science Foundation grant MCB-9507393 (to E.L.N.), by the University of Georgia Research Foundation, Inc. (to E.L.N.), and by the Administration for Economic Development of the government of Puerto Rico (to C.E.R.-A.).

We gratefully acknowledge L. S. Collier for the construction and characterization of plasmid pBAC12 and strain ACN10. In addition, we thank J. Huang for assistance with sequencing and footprinting and L. N. Ornston for helpful discussions.

REFERENCES

1. **Bradford, M. M.** 1976. A rapid and sensitive method for the quantitation of microgram quantities of protein utilizing the principle of protein-dye binding. Anal. Biochem. **72:**248–254.
2. **Canovas, J. L., and R. Y. Stanier.** 1967. Regulation of the enzymes of the β-ketoadipate pathway in *Moraxella calcoaceticus*. Eur. J. Biochem. **1:**289–300.
3. **Coco, W. M., M. R. Parsek, and A. M. Chakrabarty.** 1994. Purification of the LysR family regulator, ClcR, and its interaction with the *Pseudomonas putida clcABD* chlorocatechol operon promoter. J. Bacteriol. **176:**5530–5533.
4. **Coco, W. M., R. K. Rothmel, S. Henikoff, and A. M. Chakrabarty.** 1993. Nucleotide sequence and initial functional characterization of the *clcR* gene encoding a LysR family activator of the *clcABD* chlorocatechol operon in *Pseudomonas putida*. J. Bacteriol. **175:**417–427.
5. **Delic, I., P. Robbins, and J. Westpheling.** 1992. Direct repeat sequences are implicated in the regulation of two *Streptomyces* chitinase promoters that are subject to carbon catabolite control. Proc. Natl. Acad. Sci. USA **89:**1885–1889.
6. **Devereaux, J., P. Haeberli, and O. Smithies.** 1984. A comprehensive set of sequence analysis programs for the VAX. Nucleic Acids Res. **12:**387–395.
7. **Eraso, J. M., and S. Kaplan.** 1994. *prrA*, a putative response regulator involved in oxygen regulation of photosynthetic gene expression in *Rhodobacter sphaeroides*. J. Bacteriol. **176:**32–43.
8. **Fried, M., and D. M. Crothers.** 1981. Equilibria and kinetics of *lac* repressor operator interactions by polyacrylamide gel electrophoresis. Nucleic Acids Res. **9:**6505–6529.
9. **Genilloud, O., M. C. Garrido, and F. Moreno.** 1984. The transposon Tn5 carries a bleomycin-resistance element. Gene (Amsterdam) **32:**225–234.
10. **Goethals, K., M. van Montagu, and M. Holsters.** 1992. Conserved motifs in a divergent nod box of *Azorhizobium caulinodans* ORS571 reveal a common structure in promoters regulated by LysR-type proteins. Proc. Natl. Acad. Sci. USA **89:**1646–1650.
11. **Gralla, J.** 1985. Rapid "footprinting" on supercoiled DNA. Proc. Natl. Acad. Sci. USA **82:**3078–3081.
12. **Henikoff, S., G. W. Haughn, J. M. Calvo, and J. C. Wallace.** 1988. A large family of bacterial activator proteins. Proc. Natl. Acad. Sci. USA **85:**6602–6606.
13. **Houghton, J. E., T. M. Brown, A. J. Appel, E. J. Hughes, and L. N. Ornston.** 1995. Discontinuities in the evolution of *Pseudomonas putida cat* genes. J. Bacteriol. **177:**401–412.
14. **Huang, J., and M. A. Schell.** 1991. In vivo interactions of the NahR transcriptional activator with its target sequences. J. Biol. Chem. **266:**10830–10838.
15. **Juni, E.** 1972. Interspecies transformation of *Acinetobacter*: genetic evidence

for a ubiquitous genus. J. Bacteriol. **112:**917–931.
16. **Juni, E., and A. Janik.** 1969. Transformation of *Acinetobacter calcoaceticus* (*Bacterium anitratum*). J. Bacteriol. **98:**281–288.
17. **Kalb, V., and R. Bernlohr.** 1977. A new spectrophotometric assay for proteins in cell extracts. Anal. Biochem. **82:**362–371.
18. **Kaphammer, B., J. J. Kukor, and R. H. Olsen.** 1990. Regulation of *tfdCDEF* by *tfdR* of the 2,4-dichlorophenoxyacetic acid degradation plasmid pJP4. J. Bacteriol. **172:**2280–2286.
19. **Kaphammer, B., and R. H. Olsen.** 1990. Cloning and characterization of *tfdS*, the repressor-activator gene of *tfdB*, from the 2,4-dichlorophenoxyacetic acid catabolic plasmid pJP4. J. Bacteriol. **172:**5856–5862.
20. **Keen, N. T., S. Tamaki, D. Kobayashi, and D. Trollinger.** 1988. Improved broad-host-range plasmids for DNA cloning in gram-negative bacteria. Gene **70:**191–197.
21. **Kikuchi, Y.** GenBank accession no. D38633.
22. **Leveau, J. H., W. M. de Vos, and J. R. van der Meer.** 1994. Analysis of the binding site of the LysR-type transcriptional activator TcbR on the *tcbR* and *tcbC* divergent promoter sequences. J. Bacteriol. **176:**1850–1856.
23. **Livrelli, V., I. W. Lee, and A. O. Summers.** 1993. In vivo DNA-protein interactions at the divergent mercury resistance (*mer*) promoters. 1. Metalloregulatory protein MerR mutants. J. Biol. Chem. **268:**2623–2631.
24. **Matrubutham, U., and A. R. Harker.** 1994. Analysis of duplicated gene sequences associated with *tfdR* and *tfdS* in *Alcaligenes eutrophus* JMP134. J. Bacteriol. **176:**2348–2353.
25. **Mead, D. A., E. S. Skorupa, and B. Kemper.** 1985. Single stranded DNA SP6 promoter plasmids for engineering mutant RNA's and proteins: synthesis of a 'stretched' parathyroid hormone. Nucleic Acids Res. **13:**1103–1108.
26. **Miller, J. H.** 1972. Experiments in molecular genetics. Cold Spring Harbor Laboratory, Cold Spring Harbor, N.Y.
27. **Neidle, E. L., L. S. Collier, and G. Gaines.** Unpublished data.
28. **Neidle, E. L., C. Hartnett, and L. N. Ornston.** 1989. Characterization of *Acinetobacter calcoaceticus catM*, a repressor gene homologous in sequence to transcriptional activator genes. J. Bacteriol. **171:**5410–5421.
29. **Neidle, E. L., and L. N. Ornston.** 1987. Benzoate and muconate, structurally dissimilar metabolites, induce expression of *catA* in *Acinetobacter calcoaceticus*. J. Bacteriol. **169:**414–415.
30. **Neidle, E. L., M. K. Shapiro, and L. N. Ornston.** 1987. Cloning and expression of *Acinetobacter calcoaceticus* genes for benzoate degradation. J. Bacteriol. **169:**5496–5503.
31. **Ngai, K.-L., E. L. Neidle, and L. N. Ornston.** 1990. Catechol and chlorocatechol 1,2-dioxygenases. Methods Enzymol. **188:**120–126.
32. **Ornston, L. N.** 1966. The conversion of catechol and protocatechuate to β-ketoadipate by *Pseudomonas putida*. III. Enzymes of the catechol pathway. J. Biol. Chem. **241:**3795–3799.
33. **Ornston, L. N., and E. L. Neidle.** 1991. Evolution of genes for the β-ketoadipate pathway in *Acinetobacter calcoaceticus*, p. 201–237. *In* K. J. Towner, E. Bergogne-Berezin, and C. A. Fewson (ed.), The biology of *Acinetobacter*. Plenum Press, New York.
34. **Parsek, M. R., D. L. Shinabarger, R. K. Rothmel, and A. M. Chakrabarty.** 1992. Roles of CatR and *cis*,*cis*-muconate in activation of the *catBC* operon, which is involved in benzoate degradation in *Pseudomonas putida*. J. Bacteriol. **174:**7798–7806.
35. **Parsek, M. R., R. W. Ye, P. Pun, and A. M. Chakrabarty.** 1994. Critical nucleotides in the interaction of a LysR-type regulator with its target promoter region: *catBC* promoter activation by CatR. J. Biol. Chem. **269:**11279–11284.
36. **Prentki, P., and H. M. Krisch.** 1984. In vitro insertional mutagenesis with a selectable DNA fragment. Gene **29:**303–313.
37. **Rothmel, R. K., T. L. Aldrich, J. E. Houghton, W. M. Coco, L. N. Ornston, and A. M. Chakrabarty.** 1990. Nucleotide sequencing and characterization of *Pseudomonas putida catR*: a positive regulator of the *catBC* operon is a member of the LysR family. J. Bacteriol. **172:**922–931.
38. **Rothmel, R. K., D. L. Shinabarger, M. R. Parsek, T. L. Aldrich, and A. M. Chakrabarty.** 1991. Functional analysis of the *Pseudomonas putida* regulatory protein CatR: transcriptional studies and determination of the CatR DNA-binding site by hydroxyl-radical footprinting. J. Bacteriol. **173:**4717–4724.
39. **Sambrook, J., E. F. Fritsch, and T. Maniatis.** 1989. Molecular cloning: a laboratory manual, 2nd ed. Cold Spring Harbor Laboratory Press, Cold Spring Harbor, N.Y.
40. **Sasse-Dwight, A., and J. D. Gralla.** 1988. Probing the *Escherichia coli glnALN* upstream activation mechanism *in vivo*. Proc. Natl. Acad. Sci. USA **85:**8934–8938.
41. **Schell, M. A.** 1993. Molecular biology of the LysR family of transcriptional regulators. Annu. Rev. Microbiol. **47:**597–626.
42. **Schell, M. A., and E. F. Poser.** 1989. Demonstration, characterization, and mutational analysis of NahR protein binding to *nah* and *sal* promoters. J. Bacteriol. **171:**837–846.
43. **Shanley, M. S., E. L. Neidle, R. E. Parales, and L. N. Ornston.** 1986. Cloning and expression of *Acinetobacter calcoaceticus catBCDE* genes in *Pseudomonas putida* and *Escherichia coli*. J. Bacteriol. **165:**557–563.
44. **Simon, R., U. Priefer, and A. Puhler.** 1983. A broad host range mobilization system for in vivo genetic engineering: transposon mutagenesis in gram-negative bacteria. Bio/Technology **1:**37–45.
45. **Simon, R., J. Quandt, and W. Klipp.** 1989. New derivatives of transposon Tn5 suitable for mobilization of replicons, generation of operon fusions and induction of genes in gram-negative bacteria. Gene **80:**161–169.
46. **van der Meer, J. R., R. I. L. Eggen, A. J. B. Zehnder, and W. M. de Vos.** 1991. Sequence analysis of the *Pseudomonas* sp. strain P51 *tcb* gene cluster, which encodes metabolism of chlorinated catechols: evidence for specialization of catechol 1,2-dioxygenases for chlorinated substrates. J. Bacteriol. **173:**2425–2434.
47. **Viale, A. M., H. Kobayashi, T. Akazawa, and S. Henikoff.** 1991. *rcbR*, a gene coding for a member of the LysR family of transcriptional regulators, is located upstream of the expressed set of ribulose 1,5-bisphosphate carboxylase/oxygenase genes in the photosynthetic bacterium *Chromatium vinosum*. J. Bacteriol. **173:**5224–5229.
48. **Wertman, K., F. A. R. Wyman, and D. Botstein.** 1986. Host/vector interactions which affect the viability of recombinant phage lambda clones. Gene **49:**253–262.
49. **Williams, M. G., and P. Rogers.** 1987. Expression of *arg* genes of *Escherichia coli* during arginine limitation dependent upon stringent control of translation. J. Bacteriol. **169:**1644–1650.
50. **Yanisch-Perron, C., J. Vieira, and J. Messing.** 1985. Improved M13 phage cloning vectors and host strains: nucleotide sequences of the M13mp18 and pUC19 vectors. Gene **33:**103–119.